

000  
001  
002  
003  
004  
005  
006  
007  
008  
009  
010  
011  
012  
013  
014  
015  
016  
017  
018  
019  
020  
021  
022  
023  
024  
025  
026  
027  
028  
029  
030  
031  
032  
033  
034  
035  
036  
037  
038  
039  
040  
041  
042  
043  
044  
045  
046  
047  
048  
049  
050  
051  
052  
053  

# CONDITIONED INITIALIZATION FOR ATTENTION

**Anonymous authors**

Paper under double-blind review

## ABSTRACT

Transformers are a dominant architecture in modern machine learning, powering applications across vision, language, and beyond. At the core of their success lies the attention layer, where the query, key, and value matrices determine how token dependencies are captured. While considerable work has focused on scaling and optimizing Transformers, comparatively little attention has been paid to how the weights of the queries, keys and values are initialized. Common practice relies on random initialization or alternatives such as mimetic initialization, which imitates weight patterns from converged models, and weight selection, which transfers weights from a teacher model. In this paper, we argue that initialization can introduce an optimization bias that fundamentally shapes training dynamics. We propose **conditioned initialization**, a principled scheme that initializes attention weights to improve the spectral properties of the attention layer. Theoretically, we show that conditioned initialization can potentially reduce the condition number of the attention Jacobian, leading to more stable optimization. Empirically, it accelerates convergence and improves generalization across diverse applications, highlighting conditioning as a critical yet underexplored area for advancing Transformer performance. Importantly, conditioned initialization is simple to apply and integrates seamlessly into a wide range of Transformer architectures.

## 1 INTRODUCTION

Transformers (Vaswani et al., 2017) have rapidly become a cornerstone of modern machine learning, driving progress in fields as diverse as natural language processing (Vaswani et al., 2017; Zhuang et al., 2021; Zhen et al., 2022), computer vision (Dosovitskiy et al., 2020; Liu et al., 2021; Touvron et al., 2021; Carion et al., 2020), and robotics (Salzmann et al., 2020; Maiti et al., 2023). A key factor behind this versatility is the self-attention mechanism, which models interactions between tokens by comparing them pairwise and dynamically weighting their contributions. This ability to capture both long-range and global dependencies has positioned Transformers as a foundational architecture across a wide spectrum of learning tasks.

While substantial effort has been devoted to improving the efficiency, scalability, and expressiveness of attention mechanisms (Ali et al., 2021; Xiong et al., 2021b; Ding et al., 2022), relatively little focus has been placed on a more basic but equally important aspect: *how attention weights are initialized*. Initialization plays a critical role in shaping optimization landscapes of deep neural networks. Classical schemes such as Xavier (Glorot & Bengio, 2010) and Kaiming (He et al., 2015) initialization showed that carefully chosen scaling of weights at the start of training can dramatically improve gradient optimization and stability in deep networks. These insights were crucial for enabling the training of very deep architectures such as ResNets (He et al., 2016), where poor initialization could otherwise cause vanishing or exploding gradients. Yet, despite their depth and complexity, Transformers have received far less theoretical scrutiny on this front. Given that self-attention relies on query, key, and value projections whose interplay directly governs the stability of token interactions, it is natural to ask whether initialization schemes tailored specifically to attention could offer similar benefits.

Currently, Transformers typically adopt simple random initializations, without consideration of the unique structure of attention layers. Recent alternatives such as *mimetic initialization* (Trockman & Kolter, 2023), which transfers statistical patterns from converged models, and *weight selection* (Xu et al., 2023), which reuses pretrained weights from larger teacher models, highlight a growing recog-

054 nition that initialization matters. However, these methods remain heuristic and lack a principled  
 055 connection to the conditioning of the attention mechanism itself.  
 056

057 In this work, we revisit Transformer initialization from a theoretical perspective. We show that the  
 058 stability of optimization in self-attention layers is closely tied to the conditioning of their Jacobians,  
 059 which in turn depends on the spectral properties of the query, key, and value projections. Building  
 060 on this insight, we introduce **conditioned initialization**, a principled scheme designed to improve  
 061 the spectral conditioning of attention blocks at the start of training. Rather than directly modifying  
 062 training objectives, our method intervenes at initialization, providing an inductive bias that promotes  
 063 more stable optimization dynamics.  
 064

Our contributions are threefold:

- 065 **Theoretical framework:** We establish a connection between the conditioning of self-  
 066 attention Jacobians and the spectral structure of the query, key, and value matrices, mo-  
 067 tivating initialization schemes that explicitly target this property.  
 068
- 069 **Conditioned initialization:** We propose a simple initialization method that reduces the  
 070 upper bound on the attention Jacobian’s condition number, thereby biasing training toward  
 071 stable optimization.  
 072
- 073 **Empirical validation:** Through experiments on diverse benchmarks, spanning image clas-  
 074 sification, object detection, instance segmentation, language modeling, and long-range se-  
 075 quence learning, we show that conditioned initialization consistently accelerates conver-  
 076 gence and improves generalization, and can be easily integrated into a variety of different  
 077 Transformer architectures.  
 078

079 By highlighting initialization as a critical yet underexplored component of Transformer design, our  
 080 work opens up a new perspective on how principled conditioning can be leveraged to improve opti-  
 081 mization stability and downstream performance.  
 082

## 083 2 RELATED WORK

084 **Initialization.** Initialization strategies play a pivotal role in determining how efficiently deep net-  
 085 works can be trained. Early advances such as Xavier (Glorot & Bengio, 2010) and Kaiming initia-  
 086 lization (He et al., 2015) demonstrated that properly scaling weights at the outset helps preserve vari-  
 087 ance across layers, preventing issues like vanishing or exploding gradients. These ideas were foun-  
 088 dational in enabling the successful training of very deep architectures, most notably ResNets (He  
 089 et al., 2016). In the context of Transformers, however, initialization has typically been treated in  
 090 a more ad hoc manner, with standard practice relying on simple schemes from normal or trun-  
 091 cated normal distributions. More recent efforts have begun to acknowledge the unique structure of  
 092 attention layers. For example, mimetic initialization (Trockman & Kolter, 2023) introduces induc-  
 093 tive bias by imitating the statistical patterns of trained networks, while weight selection (Xu et al.,  
 094 2023) transfers weights from larger pretrained teacher models to provide a stronger starting point  
 095 for smaller architectures. In our experiments we compare to these two methods.  
 096

097 **Conditioning.** A growing body of work has underscored the importance of conditioning for both  
 098 the trainability and generalization of neural networks. In particular, Saratchandran et al. (2025)  
 099 showed that networks with better-conditioned weights tend to achieve superior performance, and  
 100 proposed a matrix preconditioning method to explicitly control condition numbers during training.  
 101 From a different angle, Liu et al. (2022) analyzed optimization through the lens of the neural tangent  
 102 kernel (NTK), demonstrating that well-conditioned NTKs lead to faster and more reliable conver-  
 103 gence, particularly in the infinite-width regime where the NTK dominates learning dynamics (Jacot  
 104 et al., 2018). This has been extended to the transformer setting in Yang (2020). Other studies have  
 105 pointed out structural factors that affect conditioning. For example, Agarwal et al. (2021) observed  
 106 that increasing network depth can itself improve conditioning, thereby aiding gradient-based meth-  
 107 ods. In the case of Transformers, Ji et al. (2025) argued that skip connections act as an implicit  
 108 conditioning mechanism, stabilizing the optimization of deep Transformers. Our work departs from  
 109 these approaches by asking whether initialization itself can be designed to yield better-conditioned  
 110 attention layers from the outset.  
 111

108 

### 3 THEORETICAL FRAMEWORK

109 

#### 3.1 PRELIMINARIES

110 For the theoretical framework we will primarily focus on self-attention, which is one of the most  
111 common forms of attention in a Transformer. Self-attention is composed of three learnable matrices,  
112 query  $W_Q \in \mathbb{R}^{D \times d}$ , key  $W_K \in \mathbb{R}^{D \times d}$ , and value  $W_V \in \mathbb{R}^{D \times d}$  defined for an input sequence  
113  $X \in \mathbb{R}^{N \times D}$ .

114 
$$A(X) = \text{softmax}(XW_QW_K^TX^T)XW_V \quad (1)$$

115 where softmax is the softmax activation that acts row-wise on a matrix (Prince, 2023). Note that  
116 then  $A(X) \in \mathbb{R}^{N \times d}$ . In general, Transformers employ multiple heads i.e. attention matrices  $A_i$   
117 for  $1 \leq i \leq h$  where  $h$  is the number of heads. These are then concatenated together to form a  
118 multi-head attention layer  $[A_1, \dots, A_h]$ . We point out that in some references the notation  $A(X)$  is  
119 reserved for only the term  $\text{softmax}(XW_QW_K^TX^T)$ . However, in this paper as we will be concerned  
120 with the whole attention layer we use  $A(X)$  to denote the whole layer output as defined in eq. (1).  
121 For further details on Transformers readers may consult Prince (2023).  
122123 The self-attention map of a layer in a Transformer  $A(X)$  has parameters given by those parameters  
124 in  $X$  from the previous layer and those given by  $W_Q, W_K, W_V$  that define  $A(X)$ . Our work will  
125 consider the Jacobian of  $A(X)$  with respect to the parameters within the layer of  $A(X)$ , namely  
126  $W_Q, W_K, W_V$ . Therefore, when we speak of the Jacobian of  $A(X)$  it will be with respect to  $W_Q$ ,  
127  $W_K, W_V$ . We will denote this Jacobian by  $J(A(X))$  and note that it is defined by  
128

129 
$$J(A(X)) = \left[ \frac{\partial A(X)}{\partial W_Q}, \frac{\partial A(X)}{\partial W_K}, \frac{\partial A(X)}{\partial W_V} \right]^T \quad (2)$$

130 Given a matrix  $Z \in \mathbb{R}^{m \times n}$  we denote the vectorization of  $Z$  by  $\text{vec}(Z) \in \mathbb{R}^{mn \times 1}$  (Magnus &  
131 Neudecker, 2019). Note that for such a matrix there is a transformation  $T_{mn} \in \mathbb{R}^{mn \times mn}$  such that  
132  $T_{mn}\text{vec}(Z) = \text{vec}(Z^T)$  where  $Z^T$  denotes the transpose of  $Z$ . The matrix  $T_{mn}$  is known as a  
133 commutation matrix and is a permutation matrix (Magnus & Neudecker, 2019). The maximum singular  
134 value of a matrix  $Z$  will be denoted by  $\sigma_{\max}(Z)$  and the minimum singular value by  $\sigma_{\min}(Z)$ .  
135 We will use the standard terminology SVD to denote the singular value decomposition of a matrix.  
136 Given a vector  $v \in \mathbb{R}^n$  the notation  $\|v\|_2$  will denote the vector 2-norm of  $v$ . Finally, we will let  
137  $I_{m \times n}$  denote the rectangular identity matrix that has all 1's on its main diagonal and  $\mathcal{O}_{m \times n}$  as the  
138 real  $m \times n$  semi-orthogonal matrices.  
139140 

#### 3.2 MAIN THEOREMS

141 In this section, we present the main theorem of the paper, which motivates the development of a sim-  
142 ple yet effective strategy, conditioned initialization, designed to reduce the condition number of the  
143 Jacobian of the attention layer at initialization. As shown in section 4, this scheme is straightforward  
144 to implement while providing significant optimization benefits.  
145146 **Definition 3.1.** Let  $Z$  be an  $N \times d$  matrix of full rank. The condition number of  $Z$ , denoted by  $\kappa$ ,  
147 is defined as

148 
$$\kappa(Z) = \frac{\sigma_{\max}(Z)}{\sigma_{\min}(Z)} \quad (3)$$

149 where  $\sigma_{\max}(Z)$  denotes the maximum singular value of  $Z$  and  $\sigma_{\min}(Z)$  the minimum singular value  
150 of  $Z$ , which we know is non-zero as  $Z$  is full rank.  
151152 Our objective is to analyze the condition number of the self-attention layer in a Transformer. We  
153 show that the condition number of its Jacobian depends on the condition numbers of the query, key,  
154 and value weight matrices. Furthermore, we demonstrate that initializing  $W_Q, W_K$ , and  $W_V$  with  
155 low condition numbers imparts an inductive bias into the Transformer architecture that leads to more  
156 effective optimization.  
157158 We begin by examining the derivatives of the self-attention layer with respect to the parameters  $W_Q$ ,  
159  $W_K$ , and  $W_V$ . We will need the following lemma.  
160

162  
163  
164  
165  
166

**Lemma 3.1.** Let  $\Lambda : \mathbb{R}^n \rightarrow \mathbb{R}^{n \times n}$  denote the function  $\Lambda(z) = \text{Diag}(z) - z \cdot z^T$ . We then have that

$$\frac{\partial \text{softmax}}{\partial x}(z) = \Lambda(\text{softmax}(z)). \quad (4)$$

167

**Proposition 3.1.** Let  $\mathbf{A}(X)$  denote a self-attention matrix with input  $X$  as defined by eq. (1). Then

168  
169  
170  
171

$$\frac{\partial \mathbf{A}(X)}{\partial W_Q} = (W_V^T X^T \otimes I_N) \left( \Lambda(\text{softmax}(X W_Q W_K^T X^T)) \right) (X W_K \otimes X) \quad (5)$$

172  
173

$$\frac{\partial \mathbf{A}(X)}{\partial W_K} = (W_V^T X^T \otimes I_N) \left( \Lambda(\text{softmax}(X W_Q W_K^T X^T)) \right) (X \otimes X W_Q) \cdot T_{Dd} \quad (6)$$

174  
175

$$\frac{\partial \mathbf{A}(X)}{\partial W_V} = I_d \otimes \text{softmax}(X W_Q W_K^T X^T) X \quad (7)$$

176  
177  
178

where  $\Lambda$  is defined in lemma 3.1 and  $T_{Dd}$  is the commutation matrix satisfying  $T_{Dd} \text{vec}(W_K) = \text{vec}(W_K^T)$  (see section 3.1).

179  
180

From proposition 3.1 we obtain a bound on the condition number of the Jacobian of the attention matrix.

181  
182  
183  
184

**Theorem 3.1.** Let  $\mathbf{A}(X)$  denote a self-attention matrix, as defined in eq. (1), with input  $X$  and let  $J(\mathbf{A}(X))$  denote its Jacobian with respect to the parameter matrices  $W_Q$ ,  $W_K$  and  $W_V$  as defined in eq. (2). Assume that  $J(\mathbf{A}(X))$  has full rank so that  $\kappa(J(\mathbf{A}(X)))$  is finite. Then

185  
186  
187

$$\begin{aligned} \kappa(J(\mathbf{A}(X))) \leq & \kappa(X)^3 \kappa(\Lambda(\text{softmax}(X W_Q W_K^T X^T))) \kappa(W_V) (\kappa(W_Q) + \kappa(W_K)) \\ & + \kappa(X) \kappa(\text{softmax}(X W_Q W_K^T X^T)) \end{aligned} \quad (8)$$

188  
189

where  $\Lambda$  is defined in lemma 3.1.

190  
191  
192  
193

Theorem 3.1 shows that  $\kappa(J(\mathbf{A}(X)))$  is bounded above by a sum of two terms:

$$\kappa(X)^3 \cdot \kappa(\Lambda(\text{softmax}(X W_Q W_K^T X^T))) \kappa(W_V) (\kappa(W_Q) + \kappa(W_K)) \quad (9)$$

$$\kappa(\text{softmax}(X W_Q W_K^T X^T)) \quad (10)$$

194  
195  
196  
197  
198

**Observation.** Theorem 3.1 provides a strategy for reducing the condition number of the Jacobian of  $\mathbf{A}$  through the upper bound in eq. (8). Since we directly control  $W_Q$ ,  $W_K$ , and  $W_V$ , reducing their condition numbers decreases the term in eq. (9), thereby tightening the bound. Our next step is to show that this can be achieved at initialization and to confirm empirically in section 4 that it introduces a bias which improves both optimization and performance.

199  
200

### 3.3 CONDITIONED INITIALIZATION

201  
202  
203  
204

Our goal in this section is to design a simple and effective initialization for the query, key, and value matrices  $W_Q$ ,  $W_K$ , and  $W_V$  that lowers the condition number of their singular value spectra, thereby improving the conditioning of the Jacobian  $J(\mathbf{A})$ .

205  
206

We begin with two key observations. There are two families of  $m \times n$  matrices with condition number 1:

207  
208  
209

1. scalar multiples of the identity  $\lambda I_{m \times n}$  with  $\lambda \neq 0$ , and
2. semi-orthogonal matrices  $\mathcal{O}_{m \times n}$  (matrices with orthonormal rows or columns).

210  
211  
212  
213

From theorem 3.1, the condition number of  $J(\mathbf{A})$  admits the surrogate upper bound

$$\mathcal{B}(J(\mathbf{A})) := \kappa(X)^3 \kappa(\Lambda(\text{softmax}(X W_Q W_K^T X^T))) \kappa(W_V) (\kappa(W_Q) + \kappa(W_K)) \quad (11)$$

$$+ \kappa(X) \kappa(\text{softmax}(X W_Q W_K^T X^T)). \quad (12)$$

214  
215

Unlike the true condition number  $\kappa(J(\mathbf{A}))$ , the bound  $\mathcal{B}(J(\mathbf{A}))$  can be directly influenced at initialization by controlling the conditioning of  $W_Q$ ,  $W_K$ , and  $W_V$ . Standard practice initializes these matrices from Gaussian or uniform distributions, which do not enforce good conditioning.

216 The following proposition shows that initializing  $W_Q$ ,  $W_K$ , and  $W_V$  from either of the families  
 217 above yields a strictly better surrogate bound at initialization.  
 218

219 **Proposition 3.2.** *Let  $A(X)$  denote an attention matrix with  $W_Q$ ,  $W_K$ , and  $W_V$  initialized from  
 220 a Gaussian or uniform distribution, and let  $\bar{A}(X)$  denote one where  $\bar{W}_Q$ ,  $\bar{W}_K$ , and  $\bar{W}_V$  are  
 221 initialized from either  $\{\lambda I_{D \times d}\}$  or  $\mathcal{O}_{D \times d}$ . Then*

$$222 \quad \mathcal{B}(J(\bar{A})) \leq \mathcal{B}(J(A)).$$

225 **Remark.** The quantity  $\mathcal{B}(J(A))$  is only an upper bound on  $\kappa(J(A))$ . Thus, proposition 3.2 guarantees  
 226 a tighter bound but does not by itself imply improved conditioning of the Jacobian. Nonetheless,  
 227 as we demonstrate in section 4, the initialization in proposition 3.2 consistently lowers the condition  
 228 number during training and leads to more stable optimization and improved performance.  
 229

230 **Initialization Strategy.** Although proposition 3.2 shows that initializing the matrices  $W_Q$ ,  $W_K$ ,  
 231 and  $W_V$  using either  $\{\lambda I_{D \times d}\}$  or  $\mathcal{O}_{D \times d}$  can potentially lower the condition number of  $J(A)$ , it does  
 232 not specify which choice is most suitable for each matrix. We note that  $W_Q$ ,  $W_K$ , and  $W_V$  play  
 233 distinct algebraic roles in attention, and this motivates different treatments. For the value map  $W_V$ ,  
 234 which enters linearly into the output

$$235 \quad (\text{softmax}(XW_QW_K^TX^T))(XW_V),$$

236 initializing with the rectangular identity preserves the scale of the input representations ( $XW_V =$   
 237  $X$ ), keeps  $\kappa(W_V) = 1$ , and avoids unnecessary distortion of the Jacobian. In contrast, the query  
 238 and key maps interact bilinearly through

$$239 \quad S = XW_QW_K^TX^T,$$

241 and initializing them as rectangular identities can bias projections toward coordinate subspaces,  
 242 yielding anisotropic logits and unstable softmax dynamics. A semi-orthogonal initialization for  $W_Q$   
 243 and  $W_K$  instead provides near-isometric embeddings, giving each head balanced representations of  
 244  $X$  and supporting more diverse and stable attention patterns.  
 245

246 **Implementation.** Following the above design principle, in the experiments of section 4 we  
 247 initialized the value matrices  $W_V$  for each head as rectangular identities. For the queries and keys,  
 248 we initialized each  $W_Q^{(i)}$  and  $W_K^{(i)}$  in the  $i$ -th head with independent semi-orthogonal projections,  
 249

$$250 \quad (W_Q^{(i)})^T W_Q^{(i)} = I_d, \quad (W_K^{(i)})^T W_K^{(i)} = I_d,$$

252 for  $i = 1, \dots, h$ , where  $h$  is the number of heads. This produces near-isometric embeddings into  
 253 distinct subspaces, thereby diversifying the logits  $S^{(i)} = (XW_Q^{(i)})(XW_K^{(i)})^T$  and the resulting  
 254 attention patterns. See section A.1.1 for a concrete way to carry out this procedure. We refer to  
 255 this initialization as **conditioned initialization**.  
 256

257 **Different forms of attention.** The formulation in section 3.1 describes the classical self-attention  
 258 layer used in Transformers. In practice, many recent architectures have proposed variations of attention  
 259 to improve efficiency and effectiveness (Touvron et al., 2021; Ali et al., 2021; Liu et al., 2021;  
 260 Ding et al., 2022; Xiong et al., 2021b). In particular, many of these newer forms of attention apply  
 261 normalization to the query, key and values. Our conditioned initialization is readily applicable to  
 262 these generalized forms of attention, including those with normalization (see Henry et al. (2020);  
 263 Dehghani et al. (2023); Zhang & Sennrich (2019)), and we empirically demonstrate in section 4 that  
 264 it consistently yields strong performance.  
 265

## 266 4 EXPERIMENTS

268 In this section, we evaluate the theoretical insights from section 3 across a range of Transformer  
 269 applications. For each setting, we compare our conditioned initialization against the standard de-  
 270 fault schemes commonly used in the literature, as well as more recent alternatives such as mimetic

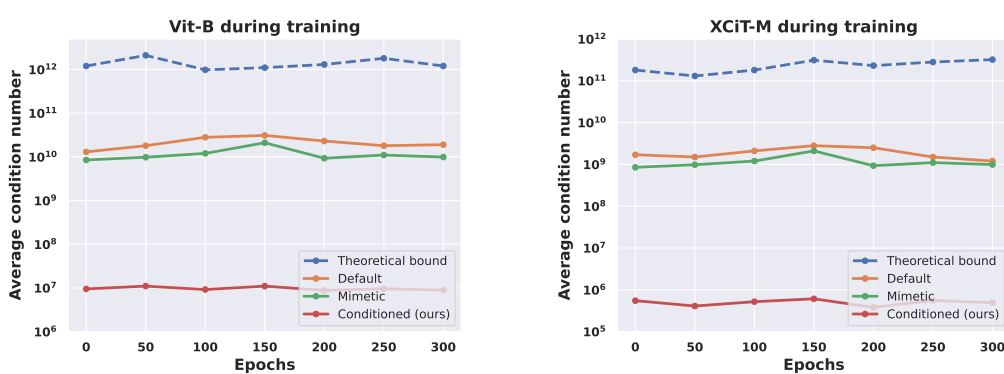


Figure 1: Average condition number of the attention Jacobian during training under three common initialization schemes, shown alongside the theoretical bound from eq. (8).

initialization (Trockman & Kolter, 2023) and weight selection (Xu et al., 2023). In all experiments, conditioned initialization is implemented as described in section 3.3. The goal is to test our initialization on a wide range of architectures at different parameter levels. For larger scale experiments we refer the reader to section A.4.

#### 4.1 VITs FOR IMAGE CLASSIFICATION

**Vision Transformers.** We applied conditioned initialization to the attention layer of a variety of modern vision Transformers: a ViT-Base (ViT-B) (Dosovitskiy et al., 2020), a Swin-Base (Swin-B) (Liu et al., 2021), a XCiT-Medium (XCiT-M) (Ali et al., 2021), a DeiT-Base (DeiT-B) (Touvron et al., 2021), and a DaViT-Base (DaViT-B) (Ding et al., 2022) for image classification on ImageNet-1k. Each model is initialized in three ways: (i) the default truncated normal initialization (Hugging Face, 2025b), (ii) mimetic initialization (Trockman & Kolter, 2023), and (iii) our conditioned initialization from section 3.3. We point out that each of these vision Transformers uses a different attention layers to the standard self-attention used in the ViT-B architecture. However, as mentioned in section 3.3 conditioned initialization applies to more general forms of attention.

**Results on ImageNet-1k.** We trained three versions of each Transformer: a baseline model with a default initialization (Hugging Face, 2025b), one with mimetic initialization (Trockman & Kolter, 2023) and one incorporating conditioned initialization, see section A.3.1 for training details. The final results, summarized in table 1, show the test accuracy for each initialization on each model. We observe that in every case, conditioned initialization outperforms the other two.

**Validating the theory.** We validate the theoretical results of section 3 using ViT-B and XCiT-M models trained on ImageNet-1k. Figure 1 reports the average condition number of the Jacobian of the attention matrices for ViT-B (left) and XCiT-M (right), during training, under the above mentioned three initializations, alongside the theoretical upper bound from theorem 3.1. The results demonstrate that conditioned initialization consistently yields a better-conditioned Jacobian, providing empirical support for its role in enabling more stable attention mechanisms.

Table 1: Comparison of Vision Transformers with different initializations pretrained on ImageNet-1k. We report Top-1% classification accuracy. In each case, conditioned initialization improves performance over the default and mimetic initializations.

	ViT-B	DeiT-B	Swin-B	XCiT-M	DaViT-B
Original	80.3	81.6	83.4	82.6	84.3
Mimetic	80.5	81.6	83.5	82.6	84.4
Conditioned (ours)	81.5	82.7	84.6	83.5	85.3

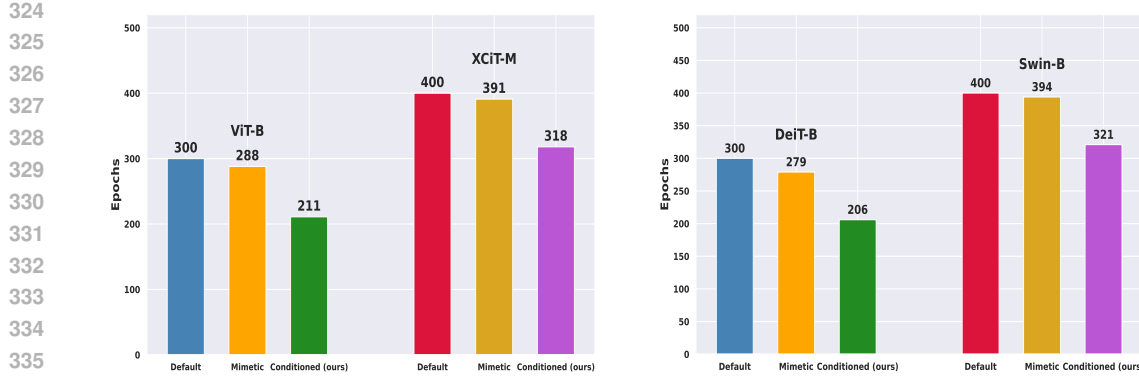


Figure 2: Total number of epochs required for each initialization to reach the final accuracy of the default initialization reported in table 1, across ViT-B, DeiT-B, Swin-B, and XCiT-M. In all cases, conditioned initialization converges more quickly, requiring fewer epochs than both default and mimetic initialization.

**Optimization efficiency.** As shown in table 1, conditioned initialization achieves higher accuracy under the same training regime compared to both default and mimetic initialization. To further assess training efficiency, we measured the number of epochs required by mimetic and conditioned initialization to match the final accuracy attained by the default initialization across ViT-B, DeiT-B, Swin-B, and XCiT-M. Figure 2 reports these results, demonstrating that conditioned initialization consistently converges 20–30% faster to the same accuracy level. Similar analysis for DaViT-B is given in section A.3.1.

#### 4.1.1 SMALL SCALE DATASETS

Following section 4.1, we assessed conditioned initialization on small-scale image classification datasets: Flowers (Nilsback & Zisserman, 2008), Pets (Vedaldi, 2012), CIFAR-10, and CIFAR-100 (Krizhevsky et al., 2009). Experiments were conducted with the ViT-Tiny (ViT-T) architecture, a common choice for such benchmarks (Trockman & Kolter, 2023; Xu et al., 2023). We compared conditioned initialization with the default truncated normal scheme (Hugging Face, 2025b) and with mimetic initialization (Trockman & Kolter, 2023). Because ViTs lack strong inductive bias, they typically perform poorly on small datasets; mimetic initialization has been shown to partially remedy this by providing a more suitable inductive bias. As shown in table 2, conditioned initialization reliably improves over the default and performs on par with mimetic initialization.

**Weight selection.** We compared our initialization with the weight selection method from Xu et al. (2023). This can be found in section A.3.1.

Table 2: Comparison of ViT-T pretrained on four small scale datasets with three different initializations. We report Top-1% classification accuracy. In each case, conditioned initialization improves performance over the default and mimetic initializations.

	Pets	Flowers	CIFAR-10	CIFAR-100
Default	26.7	64.5	92.4	71.7
Mimetic	47.7	71.6	93.6	75.0
Conditioned (ours)	47.7	72.1	94.1	75.3

#### 4.2 OBJECT DETECTION AND INSTANCE SEGMENTATION

In this section, we test conditioned initialization in a fine-tuning setting on two downstream tasks: object detection and instance segmentation. We first pretrain an XCiT architecture (Ali et al., 2021) on ImageNet-1K and then fine-tune on COCO 2017 (Lin et al., 2014). The XCiT models are used

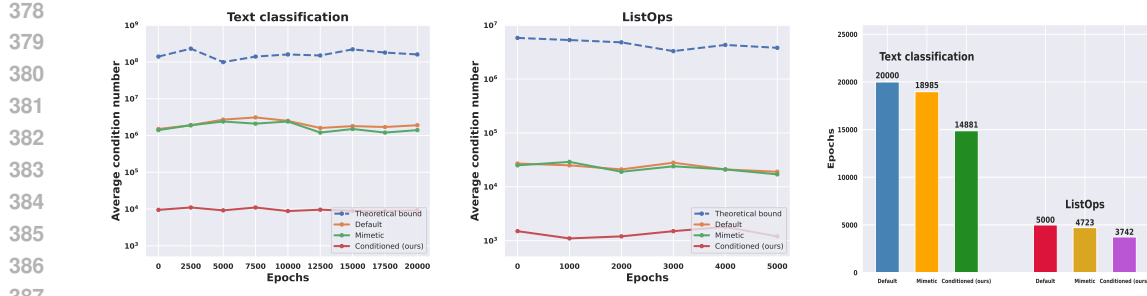


Figure 3: Average condition number of the attention Jacobian during training under three common initialization schemes, shown alongside the theoretical bound from eq. (8).

as backbones within a Mask R-CNN framework (He et al., 2017) equipped with a Feature Pyramid Network (FPN) for multi-scale features. To connect XCiT to FPN, we adapt its column structure to output intermediate representations, using the 12-layer XCiT-Small (XCiT-S) with strides adjusted from 16 to [4, 8, 16, 32] for FPN compatibility. Downsampling is done with max pooling and up-sampling with a single transposed convolution. We evaluate this setup across three initializations: default truncated normal, mimetic, and our conditioned initialization.

**Results.** The results for object detection and instance segmentation are presented in table 3. We report  $AP^b$  (Average Precision for bounding boxes),  $AP_{50/75}^b$  (Average Precision at IoU thresholds of 0.50 and 0.75 for bounding boxes),  $AP^m$  (Average Precision for masks), and  $AP_{50/75}^m$  (Average Precision at IoU thresholds of 0.50 and 0.75 for masks). Across all metrics, XCiT models with conditioned initialization consistently outperform both alternatives.

Table 3: Performance evaluation of object detection and instance segmentation on the COCO dataset. For each metric, our spectrally conditioned architecture (Spec. cond.) outperforms the original.

Model	$AP^b$	$AP_{50}^b$	$AP_{75}^b$	$AP^m$	$AP_{50}^m$	$AP_{75}^m$
Default	44.9	66.1	48.9	40.1	63.1	42.8
Mimetic	44.8	66.0	49.1	40.2	63.1	42.9
Conditioned (ours)	45.5	66.8	49.5	40.6	63.5	43.3

### 4.3 LONG RANGE SEQUENCE MODELING

Long-range sequences are essential for Transformers, enabling the integration of information across distant tokens. We assess our initialization scheme on the Long-Range Arena (LRA) benchmark (Tay et al., 2020), designed to evaluate models on extended inputs. For this, we use the Nyströmformer (Xiong et al., 2021b), which achieves efficient long-range modeling via near-linear attention. We train three variants: one with default truncated normal initialization (Xiong et al., 2021b; Hugging Face, 2025a), one with mimetic initialization (Trockman & Kolter, 2023), and one with our conditioned initialization from section 3.3 following the setup of Xiong et al. (2021b).

**Results.** From table 4 we see that across all tasks in the LRA benchmark, conditioned initialization consistently outperforms both default and mimetic initialization. We validate the theoretical results of section 3 on the text classification and ListOps task in the LRA benchmark suite. Figure 3 reports the average condition number of the Jacobian of the attention matrices for a Nyströmformer on the text classification task (left) and a Nyströmformer on the ListOps task (middle), during training, under the above mentioned three initializations, alongside the theoretical upper bound from theorem 3.1. The results demonstrate that conditioned initialization consistently yields a better-conditioned Jacobian, providing empirical support for its role in enabling more stable attention mechanisms. Furthermore, we measured the number of epochs required by mimetic and condi-

432 tioned initialization to match the final accuracy attained by the default initialization. Figure 3 (right)  
 433 reports these results demonstrating that conditioned initialization consistently converges approxi-  
 434 mately 25% faster to the same accuracy level.  
 435

436 Table 4: Nyströmformer with three different initializations on the LRA benchmark. We report  
 437 evaluation accuracy (%). As shown, our initialization improves performance across all tasks.  
 438

Model	ListOps	Text	Retrieval	Image	Pathfinder
Default	37.1	63.8	79.8	39.9	72.9
Mimetic	37.1	64.0	79.9	40.2	73.2
Conditioned (ours)	37.9	64.9	80.8	40.4	73.9

#### 446 4.4 LANGUAGE MODELING

447 We apply the insights from section 3 to the Crammed BERT language model (Geiping & Goldstein,  
 448 2023), trained with masked language modeling. We consider three variants: the original model with  
 449 default normal initialization ( $\mu = 0, \sigma = 0.02$ ), one with mimetic initialization, and one with our  
 450 conditioned initialization. All models are pretrained on The Pile (Gao et al., 2021) following the  
 451 setup of Geiping & Goldstein (2023), and evaluated on the GLUE benchmark (Wang et al., 2018).  
 452 As shown in table 5, conditioned initialization yields the strongest performance, with mimetic also  
 453 outperforming the default baseline. Additional results for GPT-2 are provided in section A.3.4.  
 454

455 Table 5: We evaluate a pretrained Crammed BERT with three different initialization schemes on the  
 456 GLUE benchmark, and find that conditioned initialization outperforms the other two.  
 457

	MNLI	SST-2	STSB	RTE	QNLI	QQP	MRPC	CoLA	Avg.
Default	83.8	92.3	86.3	55.1	90.1	87.3	85.0	48.9	78.6
Mimetic	84.1	92.5	86.5	55.1	90.3	87.5	85.1	50.1	78.9
Conditioned	84.8	92.9	86.9	55.5	91.1	87.7	86.0	51.7	79.6

## 464 5 LIMITATIONS

465 Our conditioned initialization is derived by optimizing an upper bound on the condition number of  
 466 the self-attention Jacobian, rather than minimizing the Jacobian’s condition number directly. The  
 467 motivation was to examine whether such a bound-based initialization could induce a more favorable  
 468 optimization bias for training Transformers. While this approach offers useful theoretical guidance  
 469 and is consistent with the empirical gains we observe, it remains an indirect proxy. Developing  
 470 methods that can efficiently estimate and control the exact Jacobian conditioning during training  
 471 would therefore be a valuable direction for future work.  
 472

## 473 6 CONCLUSION

474 In this paper, we introduced a theoretical framework that relates the conditioning of self-attention Ja-  
 475 cobians to the spectral properties of the query, key, and value matrices in Transformer architectures.  
 476 Building on this insight, we proposed a simple initialization strategy, conditioned initialization, that  
 477 aims to reduce the condition number of the attention Jacobian at initialization, thereby providing  
 478 a more favorable inductive bias for optimization. Extensive experiments show that this approach  
 479 consistently improves performance across a wide range of Transformer models and tasks, including  
 480 image classification, object detection, language modeling, and long-range sequence learning.<sup>1</sup>  
 481

482 <sup>1</sup>Digital tools were used for grammar and formatting only. No large language models contributed to the  
 483 research, and all findings are original work by the authors.  
 484

486 REFERENCES  
487

488 Naman Agarwal, Pranjal Awasthi, and Satyen Kale. A deep conditioning treatment of neural net-  
489 works. In *Algorithmic Learning Theory*, pp. 249–305. PMLR, 2021.

490 Alaaeldin Ali, Hugo Touvron, Mathilde Caron, Piotr Bojanowski, Matthijs Douze, Armand Joulin,  
491 Ivan Laptev, Natalia Neverova, Gabriel Synnaeve, Jakob Verbeek, et al. Xcit: Cross-covariance  
492 image transformers. *Advances in neural information processing systems*, 34:20014–20027, 2021.

493 Lukas Bossard, Matthieu Guillaumin, and Luc Van Gool. Food-101-mining discriminative compo-  
494 nents with random forests. In *European conference on computer vision*, pp. 446–461. Springer,  
495 2014.

496 Nicolas Carion, Francisco Massa, Gabriel Synnaeve, Nicolas Usunier, Alexander Kirillov, and  
497 Sergey Zagoruyko. End-to-end object detection with transformers. In *European conference on*  
498 *computer vision*, pp. 213–229. Springer, 2020.

499 Mostafa Dehghani, Josip Djolonga, Basil Mustafa, Piotr Padlewski, Jonathan Heek, Justin Gilmer,  
500 Andreas Peter Steiner, Mathilde Caron, Robert Geirhos, Ibrahim Alabdulmohsin, et al. Scaling  
501 vision transformers to 22 billion parameters. In *International conference on machine learning*,  
502 pp. 7480–7512. PMLR, 2023.

503 Mingyu Ding, Bin Xiao, Noel Codella, Ping Luo, Jingdong Wang, and Lu Yuan. Davit: Dual  
504 attention vision transformers. In *European conference on computer vision*, pp. 74–92. Springer,  
505 2022.

506 Alexey Dosovitskiy, Lucas Beyer, Alexander Kolesnikov, Dirk Weissenborn, Xiaohua Zhai, Thomas  
507 Unterthiner, Mostafa Dehghani, Matthias Minderer, Georg Heigold, Sylvain Gelly, et al. An  
508 image is worth 16x16 words: Transformers for image recognition at scale. *arXiv preprint*  
509 *arXiv:2010.11929*, 2020.

510 Ronen Eldan and Yuanzhi Li. Tinystories: How small can language models be and still speak  
511 coherent english? *arXiv preprint arXiv:2305.07759*, 2023.

512 Leo Gao, Stella Biderman, Sid Black, Laurence Golding, Travis Hoppe, Charles Foster, Jason  
513 Phang, Horace He, Aadi Thite, Eric Nabeshima, et al. The pile: An 800gb dataset of diverse  
514 text for language modeling. *arXiv preprint arXiv:2101.00027*, 2021.

515 Jonas Geiping. Cramming. <https://github.com/JonasGeiping/cramming>, 2023.

516 Jonas Geiping and Tom Goldstein. Cramming: Training a language model on a single gpu in one  
517 day. In *International Conference on Machine Learning*, pp. 11117–11143. PMLR, 2023.

518 Xavier Glorot and Yoshua Bengio. Understanding the difficulty of training deep feedforward neural  
519 networks. In *Proceedings of the thirteenth international conference on artificial intelligence and*  
520 *statistics*, pp. 249–256. JMLR Workshop and Conference Proceedings, 2010.

521 Kaiming He, Xiangyu Zhang, Shaoqing Ren, and Jian Sun. Delving deep into rectifiers: Surpassing  
522 human-level performance on imagenet classification. In *Proceedings of the IEEE international*  
523 *conference on computer vision*, pp. 1026–1034, 2015.

524 Kaiming He, Xiangyu Zhang, Shaoqing Ren, and Jian Sun. Deep residual learning for image recog-  
525 nition. In *Proceedings of the IEEE conference on computer vision and pattern recognition*, pp.  
526 770–778, 2016.

527 Kaiming He, Georgia Gkioxari, Piotr Dollár, and Ross Girshick. Mask r-cnn. In *Proceedings of the*  
528 *IEEE international conference on computer vision*, pp. 2961–2969, 2017.

529 Alex Henry, Prudhvi Raj Dachapally, Shubham Shantaram Pawar, and Yuxuan Chen. Query-key  
530 normalization for transformers. In *Findings of the Association for Computational Linguistics:*  
531 *EMNLP 2020*, pp. 4246–4253, 2020.

532 Hugging Face. Hugging face transformers — nystromformer documentation. [https://huggingface.co/docs/transformers/en/model\\_doc/nystromformer](https://huggingface.co/docs/transformers/en/model_doc/nystromformer), 2025a.  
533 Accessed: September 2025.

540 Hugging Face. Pytorch image models (timm). <https://github.com/huggingface/pytorch-image-models>, 2025b. Version 1.0.20 (or whichever you used); Apache-2.0 License.  
 541  
 542  
 543

544 Arthur Jacot, Franck Gabriel, and Clément Hongler. Neural tangent kernel: Convergence and gen-  
 545 eralization in neural networks. *Advances in neural information processing systems*, 31, 2018.  
 546  
 547 Yiping Ji, Hemanth Saratchandran, Peyman Moghadam, and Simon Lucey. Always skip attention.  
 548 *arXiv preprint arXiv:2505.01996*, 2025.  
 549  
 550 Alex Krizhevsky, Geoffrey Hinton, et al. Learning multiple layers of features from tiny im-  
 551 ages.(2009), 2009.  
 552  
 553 Tsung-Yi Lin, Michael Maire, Serge Belongie, James Hays, Pietro Perona, Deva Ramanan, Piotr  
 554 Dollár, and C Lawrence Zitnick. Microsoft coco: Common objects in context. In *Computer  
 555 Vision–ECCV 2014: 13th European Conference, Zurich, Switzerland, September 6–12, 2014,  
 556 Proceedings, Part V 13*, pp. 740–755. Springer, 2014.  
 557  
 558 Chaoyue Liu, Libin Zhu, and Mikhail Belkin. Loss landscapes and optimization in over-  
 559 parameterized non-linear systems and neural networks. *Applied and Computational Harmonic  
 560 Analysis*, 59:85–116, 2022.  
 561  
 562 Ze Liu, Yutong Lin, Yue Cao, Han Hu, Yixuan Wei, Zheng Zhang, Stephen Lin, and Baining Guo.  
 563 Swin transformer: Hierarchical vision transformer using shifted windows. In *Proceedings of the  
 564 IEEE/CVF international conference on computer vision*, pp. 10012–10022, 2021.  
 565  
 566 Jan R Magnus and Heinz Neudecker. *Matrix differential calculus with applications in statistics and  
 567 econometrics*. John Wiley & Sons, 2019.  
 568  
 569 Abhishek Maiti, Sander Oude Elberink, and George Vosselman. Transfusion: Multi-modal fusion  
 570 network for semantic segmentation. In *Proceedings of the IEEE/CVF Conference on Computer  
 571 Vision and Pattern Recognition*, pp. 6536–6546, 2023.  
 572  
 573 Matterport. Mask r-cnn implementation, 2017. URL [https://github.com/matterport/Mask\\_RCNN](https://github.com/matterport/Mask_RCNN).  
 574  
 575 Maria-Elena Nilsback and Andrew Zisserman. Automated flower classification over a large number  
 576 of classes. In *2008 Sixth Indian conference on computer vision, graphics & image processing*, pp.  
 577 722–729. IEEE, 2008.  
 578  
 579 Simon JD Prince. *Understanding deep learning*. MIT press, 2023.  
 580  
 581 Xianbiao Qi, Yelin He, Jiaquan Ye, Chun-Guang Li, Bojia Zi, Xili Dai, Qin Zou, and Rong Xiao.  
 582 Taming transformer without using learning rate warmup. *arXiv preprint arXiv:2505.21910*, 2025.  
 583  
 584 Tim Salzmann, Boris Ivanovic, Punarjay Chakravarty, and Marco Pavone. Trajectron++: Multi-  
 585 agent generative trajectory forecasting with heterogeneous data for control. *arXiv preprint  
 586 arXiv:2001.03093*, 2, 2020.  
 587  
 588 Hemanth Saratchandran, Thomas X Wang, and Simon Lucey. Weight conditioning for smooth  
 589 optimization of neural networks. In *European Conference on Computer Vision*, pp. 310–325.  
 590 Springer, 2025.  
 591  
 592 A Steiner, A Kolesnikov, X Zhai, R Wightman, J Uszkoreit, and L Beyer. How to train your  
 593 vit? data, augmentation, and regularization in vision transformers. arxiv 2021. *arXiv preprint  
 594 arXiv:2106.10270*, 5, 2016.  
 595  
 596 Yi Tay, Mostafa Dehghani, Samira Abnar, Yikang Shen, Dara Bahri, Philip Pham, Jinfeng Rao,  
 597 Liu Yang, Sebastian Ruder, and Donald Metzler. Long range arena: A benchmark for efficient  
 598 transformers. *arXiv preprint arXiv:2011.04006*, 2020.  
 599  
 600 Hugo Touvron, Matthieu Cord, Matthijs Douze, Francisco Massa, Alexandre Sablayrolles, and  
 601 Hervé Jégou. Training data-efficient image transformers & distillation through attention. In  
 602 *International conference on machine learning*, pp. 10347–10357. PMLR, 2021.

594 Asher Trockman and J Zico Kolter. Mimetic initialization of self-attention layers. In *International*  
 595 *Conference on Machine Learning*, pp. 34456–34468. PMLR, 2023.  
 596

597 Ashish Vaswani, Noam Shazeer, Niki Parmar, Jakob Uszkoreit, Llion Jones, Aidan N Gomez,  
 598 Łukasz Kaiser, and Illia Polosukhin. Attention is all you need. *Advances in neural informa-*  
 599 *tion processing systems*, 30, 2017.

600 Andrea Vedaldi. Cats and dogs. In *Proceedings of the 2012 IEEE Conference on Computer Vision*  
 601 *and Pattern Recognition (CVPR)*, pp. 3498–3505, 2012.

602

603 Alex Wang, Amanpreet Singh, Julian Michael, Felix Hill, Omer Levy, and Samuel R Bowman.  
 604 Glue: A multi-task benchmark and analysis platform for natural language understanding. *arXiv*  
 605 *preprint arXiv:1804.07461*, 2018.

606 Ross Wightman. Pytorch image models. [https://github.com/rwightman/](https://github.com/rwightman/pytorch-image-models)  
 607 *pytorch-image-models*, 2019.

608

609 Yunyang Xiong, Zhanpeng Zeng, Rudrasis Chakraborty, Fei Tan, Glenn Fung, Vikas Singh, Xi-  
 610 aodong Yuan, Sungsoo Ahn Wang, Dimitris Papailiopoulos, and Katerina Fragkiadaki. Github  
 611 repository, 2021a. URL <https://github.com/mlpen/Nystromformer>.

612 Yunyang Xiong, Zhanpeng Zeng, Rudrasis Chakraborty, Mingxing Tan, Glenn Fung, Yin Li, and  
 613 Vikas Singh. Nyströmformer: A nyström-based algorithm for approximating self-attention. In  
 614 *Proceedings of the AAAI Conference on Artificial Intelligence*, volume 35, pp. 14138–14148,  
 615 2021b.

616 Zhiqiu Xu, Yanjie Chen, Kirill Vishniakov, Yida Yin, Zhiqiang Shen, Trevor Darrell, Lingjie Liu,  
 617 and Zhuang Liu. Initializing models with larger ones. *arXiv preprint arXiv:2311.18823*, 2023.

618

619 Greg Yang. Tensor programs ii: Neural tangent kernel for any architecture. *arXiv preprint*  
 620 *arXiv:2006.14548*, 2020.

621 Biao Zhang and Rico Sennrich. Root mean square layer normalization. *Advances in neural infor-*  
 622 *mation processing systems*, 32, 2019.

623

624 Q Zhen, W Sun, H Deng, D Li, Y Wei, B Lv, J Yan, L Kong, and Y Zhong. cosformer: rethinking  
 625 softmax in attention. In *International Conference on Learning Representations*, 2022.

626

627 Liu Zhuang, Lin Wayne, Shi Ya, and Zhao Jun. A robustly optimized bert pre-training approach  
 628 with post-training. In *Proceedings of the 20th chinese national conference on computational*  
 629 *linguistics*, pp. 1218–1227, 2021.

630

631

632

633

634

635

636

637

638

639

640

641

642

643

644

645

646

647

## A APPENDIX

## ETHICS STATEMENT

This work relies solely on publicly available datasets and does not involve human subjects, personally identifiable information, or sensitive data. The proposed methods are developed exclusively to advance fundamental research in machine learning.

## REPRODUCIBILITY STATEMENT

All experiments in this work were designed with reproducibility in mind. References are provided for any external codebases employed, and full details of training protocols and hardware are described in the appendix. Complete proofs of all theoretical results are also included to allow independent verification.

## USE OF LLMs

This manuscript was prepared with the assistance of LLMs for grammar checking only. No language models were used in conducting the research or drafting the scientific content.

## A.1 THEORETICAL ANALYSIS

In this section, we give the proofs of the lemma and theorems from section 3.2 and the proposition from section 3.3.

**Notation.** For the convenience of the reader we restate the notation we used in section 3.

Given a matrix  $Z \in \mathbb{R}^{m \times n}$  we denote the vectorization of  $Z$  by  $\text{vec}(Z) \in \mathbb{R}^{mn \times 1}$  (Magnus & Neudecker, 2019). Note that for such a matrix there is a transformation  $T_{mn} \in \mathbb{R}^{mn \times mn}$  such that  $T_{mn}\text{vec}(Z) = \text{vec}(Z^T)$  where  $Z^T$  denotes the transpose of  $Z$ . The matrix  $T_{mn}$  is known as a commutation matrix and is a permutation matrix (Magnus & Neudecker, 2019). The maximum singular value of a matrix  $Z$  will be denoted by  $\sigma_{\max}(Z)$  and the minimum singular value by  $\sigma_{\min}(Z)$ . We will use the standard terminology SVD to denote the singular value decomposition of a matrix. Given a vector  $v \in \mathbb{R}^n$  the notation  $\|v\|_2$  will denote the vector 2-norm of  $v$ . Finally, we will let  $I_{m \times n}$  denote the rectangular identity matrix that has all 1's on its main diagonal. When we are dealing with square matrices we will often simply write  $I_n$  with the understanding that  $I_n$  is the  $n \times n$  square identity matrix. Context will make it clear whether we are in the square or non-square regime. We also let  $\mathcal{O}_{m \times n}$  as the real  $m \times n$  semi-orthogonal matrices.

We start with the following standard facts on derivatives of matrices. We point out to the reader that Qi et al. (2025) also computes various Jacobians of the self-attention layer using Kronecker factorizations however their computations are slightly different to ours and we therefore give explicit details of how to obtain the proofs of lemma 3.1 and proposition 3.1.

**Lemma A.1.** Let  $A \in \mathbb{R}^{n \times m}$ ,  $B \in \mathbb{R}^{k \times l}$  and  $C \in \mathbb{R}^{m \times k}$ . Then

$$\frac{\partial ACB}{\partial C} = B^T \otimes A. \quad (13)$$

*Proof.* We start by using a well known vectorization identity (Magnus & Neudecker, 2019)

$$\text{vec}(ACB) \equiv (B^T \otimes A)\text{vec}(C) \quad (14)$$

where  $\text{vec}$  denotes the vectorization operator which takes a matrix and maps it to a vector by stacking its columns on top of each other, see Magnus & Neudecker (2019). We then differentiate eq. (14) to obtain

$$\frac{\partial \text{vec}(ACB)}{\partial \text{vec}(C)} = B^T \otimes A. \quad (15)$$

The result of the lemma follows.

702 **Lemma A.2.** Let  $A \in \mathbb{R}^{n \times m}$  so that  $A^T \in \mathbb{R}^{m \times n}$ . Then

$$703 \quad \text{vec}(A^T) = T_{mn} \text{vec}(A) \quad (16)$$

$$704 \quad \frac{\partial \text{vec}(A^T)}{\partial \text{vec}(A)} = T_{mn} \quad (17)$$

705 where  $T_{mn}$  is a commutation matrix.

706 *Proof.* The first equation follows from the definition of the transpose of a matrix (Magnus & Neudecker, 2019). The second equation then follows from the first.  $\square$

707 The proof of lemma 3.1 is given as follows.

708 *Proof of lemma 3.1.* Let  $[z_1, \dots, z_n]$  denote a row vector in  $\mathbb{R}^n$ . Then by definition

$$709 \quad \text{softmax}([z_1, \dots, z_n]) = \left[ \frac{e^{z_1}}{\sum_{i=1}^n e^{z_i}}, \dots, \frac{e^{z_n}}{\sum_{i=1}^n e^{z_i}} \right]. \quad (18)$$

710 From the above equation we can compute the partial derivative and find

$$711 \quad \frac{\partial \text{softmax}(z)_i}{\partial z_j} = \text{softmax}(z)_i (\delta_{ij} - \text{softmax}(z)_j). \quad (19)$$

712 The term  $\frac{\partial \text{softmax}(z)_i}{\partial z_j}$  is precisely the  $ij$  component of the matrix  $\frac{\partial \text{softmax}(z)}{\partial z}$ . Putting each of these  $ij$  terms into an  $n \times n$  matrix we find

$$713 \quad \frac{\partial \text{softmax}(z)}{\partial z} = \text{Diag}(z) - z \cdot z^T \quad (20)$$

714 which proves the lemma.  $\square$

715 We can use the above lemmas to give the proof of proposition 3.1.

716 *Proof of proposition 3.1.* We start by establishing the derivative formula for the term  $\frac{\partial A(X)}{\partial W_Q}$ . We  
717 will use the notation used in section 3.1. Note that by definition  $\frac{\partial A(X)}{\partial W_Q} \in \mathbb{R}^{dN \times dD}$ . Using eq. (1)

$$718 \quad A(X) = I_N \text{softmax}(XW_Q W_K^T X^T) XW_V \quad (21)$$

719 where  $I_N$  is the  $N \times N$  identity matrix. This is done so that we can apply lemma A.1. We then  
720 compute

$$721 \quad \frac{\partial A(X)}{\partial W_Q} = \frac{\partial (I_N \text{softmax}(XW_Q W_K^T X^T) XW_V)}{\partial W_Q} \quad (22)$$

$$722 \quad = (W_V^T X^T \otimes I_N) \frac{\partial \text{softmax}(XW_Q W_K^T X^T)}{\partial W_Q} \text{ using lemma A.1} \quad (23)$$

$$723 \quad = (W_V^T X^T \otimes I_N) \Lambda(\text{softmax}(XW_Q W_K^T X^T)) \frac{\partial (XW_Q W_K^T X^T)}{\partial W_Q} \text{ using lemma 3.1} \quad (24)$$

$$724 \quad = (W_V^T X^T \otimes I_N) \Lambda(\text{softmax}(XW_Q W_K^T X^T))(XW_K \otimes X) \quad (25)$$

725 which proves the first equality in proposition 3.1.

726 To compute  $\frac{\partial A(X)}{\partial W_K} \in \mathbb{R}^{dN \times dD}$  we proceed in a similar way.

$$727 \quad \frac{\partial A(X)}{\partial W_K} = \frac{\partial (I_N \text{softmax}(XW_Q W_K^T X^T) XW_V)}{\partial W_K} \quad (26)$$

$$728 \quad = (W_V^T X^T \otimes I_N) \frac{\partial \text{softmax}(XW_Q W_K^T X^T)}{\partial W_K} \text{ using lemma A.1} \quad (27)$$

$$729 \quad = (W_V^T X^T \otimes I_N) \Lambda(\text{softmax}(XW_Q W_K^T X^T)) \frac{\partial (XW_Q W_K^T X^T)}{\partial W_K} \text{ using lemma 3.1} \quad (28)$$

$$730 \quad = (W_V^T X^T \otimes I_N) \Lambda(\text{softmax}(XW_Q W_K^T X^T))(X \otimes XW_Q) T_{Dd} \quad (29)$$

756 where the last equality follows from lemmas A.1 and A.2 This establishes the second equality in  
 757 proposition 3.1.

758 To prove the identity for  $\frac{\partial A(X)}{\partial W_V} \in \mathbb{R}^{dN \times dD}$  we write

$$760 \quad A(X) = \text{softmax}(XW_Q W_K^T X^T) XW_V I_d \quad (30)$$

762 where  $I_d$  is the  $d \times d$  identity matrix. Then we simply apply lemma A.1 to obtain

$$763 \quad \frac{\partial A(X)}{\partial W_V} = \frac{\partial(\text{softmax}(XW_Q W_K^T X^T) XW_V I_d)}{\partial W_V} \quad (31)$$

$$766 \quad = I_d \otimes \text{softmax}(XW_Q W_K^T X^T) X \quad (32)$$

767 which proves the final equality in proposition 3.1.  $\square$

768 We also give the proof of theorem 3.1.

770 *Proof of theorem 3.1.* The proof of theorem 3.1 follows from using proposition 3.1 and the definition  
 771 of the Jacobian of  $A(X)$  with respect to  $W_Q$ ,  $W_K$  and  $W_V$  given by

$$773 \quad J(A(X)) = \left[ \frac{\partial(A(X))}{\partial W_Q}, \frac{\partial(A(X))}{\partial W_K}, \frac{\partial(A(X))}{\partial W_V} \right]^T. \quad (33)$$

776 We recall that the condition number is defined as  $\kappa(J(A(X))) = \frac{\sigma_{\max}(J(A(X)))}{\sigma_{\min}(J(A(X)))}$  where  
 777  $\sigma_{\max}(J(A(X)))$  is the maximum singular value of  $J(A(X))$  and  $\sigma_{\min}(J(A(X)))$  the minimum  
 778 singular value which we know is non-zero because of the assumption that  $J(A(X))$  has full rank.

779 Note that, using the notation in section 3.1, we have that  $J(A(X)) \in \mathbb{R}^{3dN \times dD}$  as  $\frac{\partial A(X)}{\partial W_Q}, \frac{\partial A(X)}{\partial W_K},$   
 780  $\frac{\partial A(X)}{\partial W_V} \in \mathbb{R}^{dN \times dD}$ . For each of notation we will write  $A_Q := \frac{\partial A(X)}{\partial W_Q}, A_K := \frac{\partial A(X)}{\partial W_K}, A_V := \frac{\partial A(X)}{\partial W_V}$ .

782 We will start by computing a bound for the maximum singular value. We have for any vector  
 783  $z \in \mathbb{R}^{dD}$  we have

$$784 \quad \|J(A(X))z\|_2^2 = \left\| \left[ \frac{\partial(A(X))}{\partial W_Q}(z), \frac{\partial(A(X))}{\partial W_K}(z), \frac{\partial(A(X))}{\partial W_V}(z) \right]^T \right\|_2^2 \quad (34)$$

$$787 \quad = \| [A_Q(z), A_K(z), A_V(z)] \|_2^2 \quad (35)$$

$$789 \quad = \|A_Q(z)\|_2^2 + \|A_K(z)\|_2^2 + \|A_V(z)\|_2^2 \quad (36)$$

$$790 \quad \leq (\sigma_{\max}(A_Q)^2 + \sigma_{\max}(A_K)^2 + \sigma_{\max}(A_V)^2) \|z\|_2^2. \quad (37)$$

791 This implies that

$$793 \quad \sigma_{\max}(J(A(X))) := \max_{z \neq 0} \frac{\|J(A(X))z\|_2^2}{\|z\|_2^2} \quad (38)$$

$$795 \quad \leq \sqrt{\sigma_{\max}(A_Q)^2 + \sigma_{\max}(A_K)^2 + \sigma_{\max}(A_V)^2} \quad (39)$$

$$797 \quad \leq \sigma_{\max}(A_Q) + \sigma_{\max}(A_K) + \sigma_{\max}(A_V). \quad (40)$$

798 The next step is to compute a lower bound for the minimum singular value  $\sigma_{\min}(J(A(X)))$ . The  
 799 approach is similar to the above, using the fact that  $\sigma_{\min}(J(A(X))) = \min_{\|z\|_2=1} J(A(X))(z)$ . We  
 800 can then use the inequality

$$802 \quad \|J(A(X))z\|_2^2 = \left\| \left[ \frac{\partial(A(X))}{\partial W_Q}(z), \frac{\partial(A(X))}{\partial W_K}(z), \frac{\partial(A(X))}{\partial W_V}(z) \right]^T \right\|_2^2 \quad (41)$$

$$805 \quad \geq \max \left\{ \left\| \frac{\partial(A(X))}{\partial W_Q}(z) \right\|, \left\| \frac{\partial(A(X))}{\partial W_K}(z) \right\|, \left\| \frac{\partial(A(X))}{\partial W_V}(z) \right\| \right\} \quad (42)$$

807 Then minimizing the above over the constraint  $z \in \mathbb{R}^{dD}$  such that  $\|z\| = 1$  we obtain

$$809 \quad \sigma_{\min}(J(A(X))) \geq \max \left\{ \sigma_{\min} \left( \frac{\partial(A(X))}{\partial W_Q} \right), \sigma_{\min} \left( \frac{\partial(A(X))}{\partial W_K} \right), \sigma_{\min} \left( \frac{\partial(A(X))}{\partial W_V} \right) \right\}. \quad (43)$$

810 Combing the bounds on  $\sigma_{\max}(J(\mathbf{A}(X)))$  and  $\sigma_{\min}(J(\mathbf{A}(X)))$  we obtain  
 811

$$812 \quad \kappa(J(\mathbf{A}(X))) \leq \kappa\left(\frac{\partial(\mathbf{A}(X))}{\partial W_Q}\right) + \kappa\left(\frac{\partial(\mathbf{A}(X))}{\partial W_K}\right) + \kappa\left(\frac{\partial(\mathbf{A}(X))}{\partial W_V}\right). \quad (44)$$

813 The final step is to get a bound on the condition numbers for each term on the right hand side in the  
 814 above inequality. This is done using two facts: Firstly, given two matrices  $C$  and  $D$  such that the  
 815 product  $CD$  is full rank then  $\kappa(CD) \leq \kappa(C)\kappa(D)$  and the second that  $\kappa(C \otimes D) = \kappa(C)\kappa(D)$ .  
 816 Using these two facts we can then use proposition 3.1 to obtain the bound of theorem 3.1 and the  
 817 proof is finished.  $\square$   
 818

819 Using theorem 3.1 the proof of proposition is straightforward.  
 820

821 *Proof of proposition 3.2.* We first observe that by definition of the condition number of a general  
 822  $m \times n$  matrix  $M$  must always satisfy  $\kappa(M) \geq 1$ . For matrices with 1's on the diagonal and zero  
 823 elsewhere the condition number is 1. If  $M$  is a semi-orthogonal matrix then either  
 824

$$825 \quad 1. MM^T = I_{m \times m} \text{ if } m \geq n \quad (45)$$

$$826 \quad 2. M^T M = I_{n \times n} \text{ if } n \geq m. \quad (46)$$

827 Since the singular values of  $M$  are precisely the eigenvalues of  $MM^T$  if  $m \geq n$  or  $M^T M$  if  $n \geq m$ .  
 828 It follows that the singular values of  $M$  must all be 1 and hence it has condition number 1.  
 829

830 Therefore, if the  $W_Q$ ,  $W_K$  and  $W_V$  matrices are initialized as  $I_{D \times d}$  or as a matrix in  $\mathcal{O}_{D \times d}$  we have  
 831 that their condition number is 1. Therefore, we must have

$$832 \quad \mathcal{B}(\bar{\mathbf{A}}) \leq \mathcal{B}(\mathbf{A}) \quad (47)$$

833 and the proposition is proved.  $\square$

834 *Remark A.1.* In the implementation strategy in section 3.2 we saw that we initialized the values  
 835 matrix  $W_V$  with a rectangular identity matrix  $I_{D \times d}$ . However, from the theory of that section we  
 836 could have also initialized it with  $\lambda I_{D \times d}$  for  $\lambda \neq 0$ . In general, we found empirically that this could  
 837 be done but that if  $\lambda$  got too large we noticed some instability in training due to  $W_V$  having weights  
 838 that were too large. Therefore, opting for the identity  $I_{D \times d}$  was what we found worked well.  
 839

840 **Why Conditioning the Jacobian Aids Optimization.** The rationale for improving the conditioning  
 841 of the self-attention Jacobian is connected to established results on the Neural Tangent Kernel  
 842 (NTK). Prior work, see Liu et al. (2022), has shown that better-conditioned NTKs lead to faster  
 843 and more reliable convergence to a global minima during gradient-based optimization. Since the  
 844 singular values of a network's Jacobian correspond to the positive square roots of the eigenvalues  
 845 of its NTK, improving the conditioning of the Jacobian directly enhances the conditioning of the  
 846 NTK. This connection provides a theoretical basis for why controlling the spectral structure of the  
 847 self-attention Jacobian can benefit optimization. Furthermore, recent extensions of NTK theory to  
 848 transformer architectures (e.g., Yang 2020) support the relevance of these insights in the attention  
 849 setting. Our initialization scheme leverages this relationship by explicitly targeting improved con-  
 850 ditioning at initialization, which is consistent with the empirical performance gains observed across  
 851 tasks.

### 852 A.1.1 IMPLEMENTATION DETAILS

853 In this section, we give the details of how we implement the semi-orthogonal initialization of the  
 854  $W_Q$  and  $W_V$  matrix of each head.  
 855

856 We recall from section 3.3 that our initialization for the queries and keys, proceeded by initializing  
 857 each  $W_Q^{(i)}$  and  $W_K^{(i)}$  in the  $i$ -th head with independent semi-orthogonal projections,  
 858

$$859 \quad (W_Q^{(i)})^T W_Q^{(i)} = I_d, \quad (W_K^{(i)})^T W_K^{(i)} = I_d,$$

860 for  $i = 1, \dots, h$ , where  $h$  is the number of heads. To do this suppose each  $W_Q^{(i)}$  and  $W_K^{(i)}$  are  $D \times d$   
 861 and let  $r = \min(D, d)$  for each head we form two random matrices  $R_i^Q$  and  $R_i^K$  of shape  $D \times d$  and  
 862 then take the truncated SVD  
 863

$$U_i^Q(r)S_i^Q(r)(V_i^Q)^T(r) \text{ and } U_i^K(r)S_i^K(r)(V_i^K)^T(r) \quad (48)$$

864 where each of the  $U_i^Q(r) \in \mathbb{R}^{D \times r}$  and  $(V_i^Q)(r) \in \mathbb{R}^{r \times d}$  and similarly for the  $K$  ones. We then  
 865 observe that

$$866 \quad O_i^Q := U_i^Q(r) \cdot (V_i^Q)^T(r) \text{ and } O_i^K := U_i^K(r) \cdot (V_i^K)^T(r) \quad (49)$$

867 are semi-orthogonal. Doing this for each different head we get different semi-orthogonal matrices  
 868 for each  $W_Q$  and  $W_K$  for each head. The implementation of  $W_V$  is the same for each head and is  
 869 simply done by fixing  $W_V = I_{D \times d}$ .

870 *Remark A.2.* We note that in the above we used the SVD to obtain the initializations of each  $W_Q$   
 871 and  $W_V$ . One can also use the QR decomposition (Magnus & Neudecker, 2019) and PyTorch has a  
 872 built in way to do this via `nn.init.orthogonal`.

## 874 A.2 DISCUSSION ON NORMALIZATION

875 This section provides additional clarification on how normalization and stabilization mechanisms  
 876 interact with the Jacobian conditioning analysis and with the proposed conditioned initialization  
 877 scheme. Several modern transformer architectures apply normalization directly to the queries, keys,  
 878 or values (e.g., RMSNorm, QKNorm), while Layer Normalization (LN) is typically applied to the  
 879 inputs of each block. The discussion below outlines how these components relate to the theoretical  
 880 results in section 3 and to the practical behaviour observed in section 4.

881 **Theoretical setting.** In the original self-attention formulation Vaswani et al. (2017), no normalization  
 882 is applied directly to the query, key, or value weight matrices. The only modification is the fixed  
 883 scaling factor  $1/\sqrt{d}$ , determined by the head dimension. Since this factor does not depend on the  
 884 model parameters, differentiating the attention map simply scales the Jacobian by a constant. A con-  
 885 stant scalar multiplication does not change the condition number of a matrix; therefore, this scaling  
 886 has no effect on the conditioning analysis developed in Section 3. The derivations for vanilla self-  
 887 attention thus remain mathematically correct and serve as a foundation for the initialization scheme  
 888 proposed later.

889 **Compatibility with modern normalization layers.** Many contemporary transformer variants in-  
 890 incorporate normalization directly into the attention pathway, for example through RMSNorm or  
 891 QKNorm applied to queries, keys, or values. The conditioned initialization introduced in this paper  
 892 is designed to operate on top of these mechanisms rather than as a replacement for them. In all  
 893 experiments, the architectures retain their original normalization layers exactly as implemented in  
 894 the publicly released codebases. For example, the DeiT-B model applies QKNorm to both queries  
 895 and keys. When applying conditioned initialization, these QKNorm layers remain in place. This  
 896 ensures that comparisons in section 4 are consistent with the established baseline implementations  
 897 in the literature.

898 **Normalization versus conditioning.** Normalization and conditioning address different aspects of  
 899 stability. Normalization controls the scale of activations and gradients, whereas conditioning con-  
 900 cerns the spectral structure of the Jacobian. These effects are distinct. A matrix may have small  
 901 norm but poor conditioning, or it may have large norm yet be well-conditioned. For example,

$$904 \quad A = \begin{bmatrix} 1 & 0 \\ 0 & 1 \end{bmatrix}, \quad B = \begin{bmatrix} 10.1 & 0 \\ 0 & 10 \end{bmatrix}$$

907 have very different Frobenius norms but nearly identical condition numbers, while

$$909 \quad C = \begin{bmatrix} 1 & 0 \\ 0 & 1 \end{bmatrix}, \quad D = \begin{bmatrix} \sqrt{2} & 0 \\ 0 & 0.1 \end{bmatrix}$$

911 have similar Frobenius norms but condition numbers 1 and approximately 14.14, respectively. Nor-  
 912 malization schemes such as LN, RMSNorm, and QKNorm regulate magnitudes, while conditioned  
 913 initialization directly shapes the spectral behaviour of the Jacobian. These mechanisms therefore  
 914 complement one another.

915 **Ablation on Partial Initialization.** We conducted several ablation studies in which the condi-  
 916 tioned initialization was applied to only a subset of the attention projection matrices, such as ini-  
 917 tializing only  $W_Q$ , only  $W_K$ , or only  $W_V$ . An initial hypothesis was that initializing  $W_V$  alone

918 might be sufficient, since the softmax operation effectively performs a row-wise normalization on  
 919 the attention scores. However, normalization and conditioning target fundamentally different prop-  
 920 erties: a matrix may have small norm yet still exhibit a large condition number. This observation  
 921 led us to a more complete analysis, formalized in theorem 3.1, which shows that the conditioning of  
 922 the self-attention Jacobian depends on the joint spectral structure of  $W_Q$ ,  $W_K$ , and  $W_V$ . Consistent  
 923 with this theoretical insight, we found that applying conditioned initialization to all three projections  
 924 yields the most stable behaviour and the strongest empirical performance.

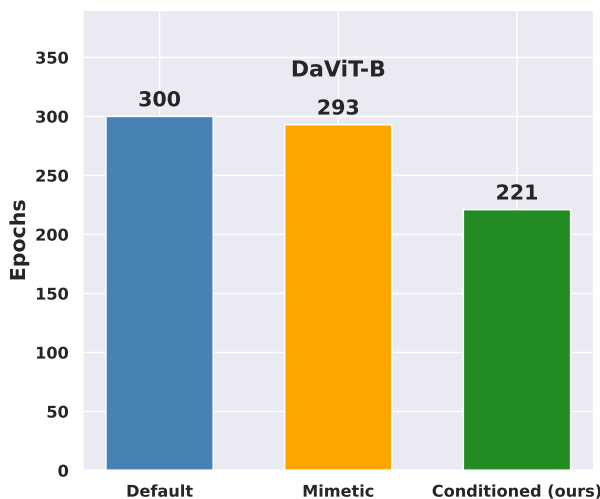
925  
 926 **Discussion on the Output Projection.** We also examined whether the conditioned initialization  
 927 should be applied to the output projection matrix  $W_O$ , given its close relationship to  $W_V$ . Empir-  
 928 ically, we found that once  $W_V$  is initialized using the proposed scheme, the initialization of  $W_O$   
 929 has negligible effect. Applying the conditioned initialization to  $W_O$  in addition to  $W_V$  did not al-  
 930 ter training behaviour or final performance. Consequently, our method focuses on conditioning the  
 931 query, key, and value projections, while leaving  $W_O$  with its standard initialization.

932 **A.3 EXPERIMENTS**

934 **A.3.1 VISION TRANSFORMERS**

936 **Hardware and implementation.** The image classification experiments in section 4.1 of the paper  
 937 were done on Nvidia A100 GPUs. The implementation of the ViTs was all done using the Timm  
 938 code base (Wightman, 2019). The architectures were all trained from scratch on the ImageNet-  
 939 1k dataset using the AdamW optimizer following the hyperparameters used in the original papers  
 940 (Dosovitskiy et al., 2020; Steiner et al., 2016; Liu et al., 2021; Ali et al., 2021; Touvron et al.,  
 941 2021; Ding et al., 2022). For the case of ViT-T on the Pets, Flowers, CIFAR-10 and CIFAR-100  
 942 datasets we used Wightman (2019) for the architecture and the training hyperparameters from Xu  
 943 et al. (2023).

944 **Optimization analysis for DaViT-B.** As shown in table 1, conditioned initialization achieves  
 945 higher accuracy under the same training regime compared to both default and mimetic initializa-  
 946 tion on the DaViT-B architecture. To further assess training efficiency, we measured the number of  
 947 epochs required by mimetic and conditioned initialization to match the final accuracy attained by the  
 948 default initialization across on the DaViT-B architecture. Figure 4 reports these results, demon-  
 949 strating that conditioned initialization consistently converges to approximately 25% faster to the same  
 950 accuracy level.



969 Figure 4: Total number of epochs required for each initialization to reach the final accuracy of  
 970 the default initialization reported in table 1 for DaViT-B architecture. Conditioned initialization  
 971 converges more quickly, requiring fewer epochs than both default and mimetic initialization.

**Weight Selection** Xu et al. (Xu et al., 2023) introduced the weight selection method, showing that weights transferred from an ImageNet-21K-pretrained ViT-Small (ViT-S) model provide a strong inductive bias for initializing a ViT-Tiny (ViT-T) on small-scale datasets. Here, we examine whether weight selection remains effective when pretraining is performed on ImageNet-1K. To this end, we pretrained ViT-S models on ImageNet-1K under three initialization schemes: default truncated normal (Hugging Face, 2025b), mimetic (Trockman & Kolter, 2023), and our conditioned initialization from section 3.3. Using the weight selection procedure (Xu et al., 2023), we then derived corresponding ViT-T initializations and trained them on Food-101 (Bossard et al., 2014), CIFAR-10, and CIFAR-100 (Krizhevsky et al., 2009). Table 6 summarizes the results. Each entry labeled “ImageNet-1K” indicates that the ViT-S model was pretrained on ImageNet-1K with the specified initialization before its weights were transferred to ViT-T via weight selection. For comparison, the final row reports the performance of a ViT-T initialized from an ImageNet-21K-pretrained ViT-S with default truncated normal initialization. The results highlight a key finding: replacing ImageNet-21K with ImageNet-1K can yield comparable performance, provided that the initialization is chosen carefully. In particular, conditioned initialization on ImageNet-1K achieves accuracy on par with default initialization pretrained on ImageNet-21K, underscoring its effectiveness in data-limited pre-training regimes.

Table 6: Comparison of ViT-T pretrained on four small scale datasets with three different initializations. We report Top-1% classification accuracy. In each case, conditioned initialization improves performance over the default and mimetic initializations.

	Food-101	CIFAR-10	CIFAR-100
ImageNet-1k + Default	85.5	96.6	79.7
ImageNet-1k + Mimetic	86.4	96.3	79.9
ImageNet-1k + Conditioned (ours)	<b>87.3</b>	<b>97.1</b>	81.0
ImageNet-21k + Default	87.1	<b>97.1</b>	<b>81.1</b>

**Training loss curves.** We plot the training curves for each of the vision transformer experiments with each different initialization. In fig. 5, fig. 6, fig. 7 we plot the training loss for the different initializations for the ViT-B, DeiT-B, Swin-B, XCiT-M and DaViT-B architectures respectively. In each case, we see conditioned initialization has trains stably and converges faster when compared to the default and Mimetic initializations.

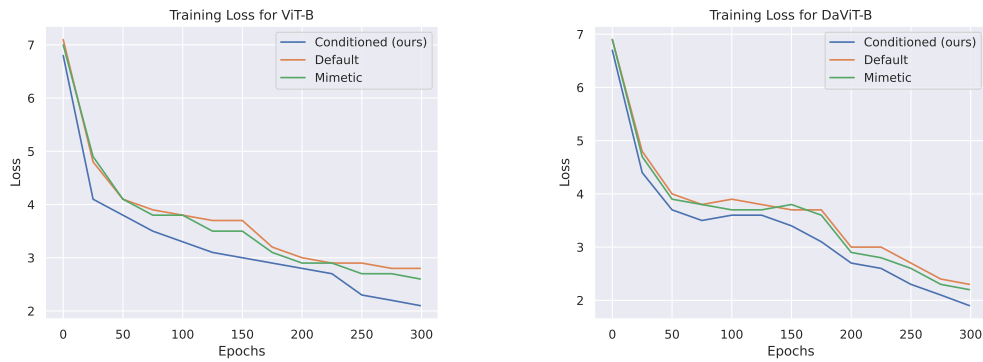


Figure 5: Training loss curves for different initializations for ViT-B (left) and DeiT-B (right).

### A.3.2 OBJECT DETECTION AND INSTANCE SEGMENTATION

**Hardware and Implementation:** The experiments for section 4.2 of the paper on object detection and instance segmentation were carried out on Nvidia A100 GPUs. The implementation followed He et al. (2017). We used the code base given by the GitHub Matterport (2017) following their exact training regime.

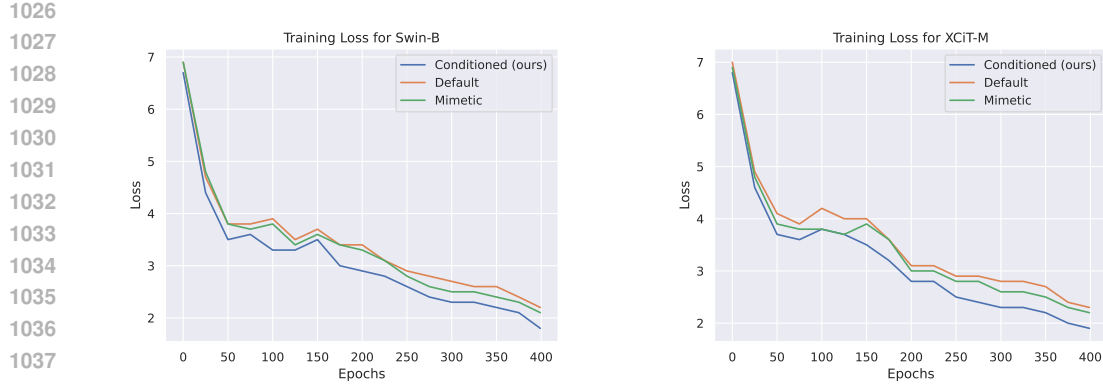


Figure 6: Training loss curves for different initializations for Swin-B (left) and XCiT-M (right).

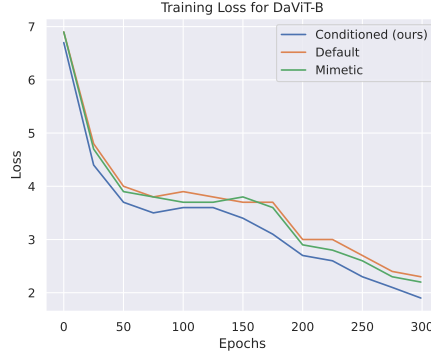


Figure 7: Training loss curves for different initializations for DaViT-B.

### A.3.3 LONG RANGE SEQUENCE MODELING WITH NYSTRÖMFORMER

**Hardware and Implementation.** All the experiments for the Nyströmformer on LRA benchmark results in section 4.3 were carried out on Nvidia A100 GPUs following the implementation and hyperparameter settings given in Xiong et al. (2021a).

### A.3.4 LANGUAGE MODELING

**Crammed BERT.** The BERT language modeling experiment in section 4.4 were all carried out on a Nvidia A6000 GPU. The Crammed-Bert was implemented following the original paper Geiping & Goldstein (2023) and the original GitHub Geiping (2023). The training regime follows Geiping (2023).

**GPT-2 on TinyStories.** We train an autoregressive Transformer, namely a GPT-2 architecture trained on the TinyStories dataset (Eldan & Li, 2023). Once again we compared three initializations: one with the default normal initialization ( $\mu = 0, \sigma = 0.02$ ), one with mimetic and a third with conditioned initialization. As shown in table 7, conditioned initialization achieves a lower perplexity than both the default and mimetic initializations showing that it boosts performance in the setting of autoregressive Transformers. We used the training regime from (Eldan & Li, 2023).

### A.4 LARGER SCALE EXPERIMENTS

In this section we tested our initialization on much larger models in both the vision and language setting.

1080 Table 7: GPT-2 models trained on the TinyStories dataset. We initialize a model in three different  
 1081 ways. Conditioned initialization achieves a perplexity than the other two initializations.  
 1082

	Perplexity
Default	2.47
Mimetic	2.40
Conditioned (ours)	2.29

1090 We ran a larger GPT-2 model, 472 million parameters, on the WikiText-103 dataset and the TinyS-  
 1091 tories dataset. The results are shown in table 8 and table 9 below clearly shows our initialization  
 1092 obtains better performance by obtaining the lowest perplexity.  
 1093

1094 Table 8: Perplexity of 472M GPT-2 model pretrained on TinyStories.  
 1095

Model	Perplexity
Default	2.39
Mimetic	2.32
Conditioned (ours)	2.20

1101 Table 9: Perplexity of 472M GPT-2 model pretrained on WikiText-103.  
 1102

Model	Perplexity
Default	44.2
Mimetic	43.8
Conditioned (ours)	42.7

1109 We repeated this experiment with a 1.72 billion parameter GPT-2 model. In this case we witnessed  
 1110 overfitting in all initialized cases. However, this is to be expected as a billion parameter model  
 1111 is too large for the TinyStories and WikiText-103 datasets. Yet even in this case our initialization  
 1112 performed much better as can be seen from table 10 and table 11.  
 1113

1114 Table 10: Perplexity of 1.72B GPT-2 model pretrained on TinyStories.  
 1115

Model	Perplexity
Default	4.15
Mimetic	4.25
Conditioned (ours)	4.03

1121 Table 11: Perplexity of 1.72B GPT-2 model pretrained on WikiText-103.  
 1122

Model	Perplexity
Default	48.1
Mimetic	48.5
Conditioned (ours)	46.9

1128 We also ran experiments on large scale ViTs on the ImageNet-1k dataset, where these models range  
 1129 from 200-300M parameters. Once again for these larger models we witnessed overfitting (this has  
 1130 also been observed in Dosovitskiy et al. (2020); Ding et al. (2022)) yet even in this case our initial-  
 1131 ization outperformed the other two standard ones, see table 12.  
 1132

1133 We then ran two 1 billion parameter models namely a ViT-Giant (ViT-G) and a DaViT-Giant (DaViT-  
 G) as these where some of the standard billion parameter vision transformers we could find in

1134 Table 12: Large scale ViTs with different initializations pretrained on ImageNet-1k. We show the  
 1135 Top1% accuracy.

	ViT-L	DeiT-L	Swin-L	XCiT-L	DaViT-L
Original	79.6	80.7	82.6	81.5	83.3
Mimetic 2	79.7	80.6	82.4	81.5	83.2
Conditioned (ours)	80.7	81.5	83.7	82.4	84.4

1142 Hugging Face (2025b). We pretrained them each with the different initializations on ImageNet-1k.  
 1143 As can be seen from table 13 our initialization out performs the other two.

1144 Table 13: 1B scale ViTs with different initializations pretrained on ImageNet-1k. We show the  
 1145 Top1% accuracy.

	ViT-G	DaViT-G
Original	78.8	81.9
Mimetic 2	78.6	82.0
Conditioned (ours)	79.9	82.9